This article has been accepted for publication in a future issue of this journal, but has not been fully edited. Content may change prior to final publication. Citation information: DOI 10.1109/TIE.2015.2395386, IEEE Transactions on Industrial Electronics

Energy Management of a Fuel Cell Serial-Parallel Hybrid System

Harrynson Ramírez-Murillo, Carlos Restrepo, Javier Calvente, *Member, IEEE,* Alfonso Romero, *Member, IEEE,* and Roberto Giral, *Senior Member, IEEE*.

***Abstract*—In this work, a serial-parallel hybrid (SPH) power system formed by a Fuel Cell (FC), an Auxiliary Storage Device (ASD) and the current-controlled dc-dc converters responsible for the power management are realized by using the Digital Signal Controller (DSC) TMS32F28335. The main energy management goal is to transfer energy from the sources (FC or ASD) to the load while ensuring dc bus voltage regulation and high power conversion efficiency. In addition, a safe and reliable operation of the system has to be achieved. The selected converter and its controller features are: non-inverting voltage step up and step down, high efficiency, input and output currents regulation an low ripple values, and the ability to change from input to output current regulation loop, suddenly and smoothly, and vice versa. All these features allow it to be positioned in different FC system localizations and simplifies the design of the master control. Simulation and experimental results have been validated on a 48-V, 1200-W dc bus.**

***Index Terms*—Current control, dc-dc power conversion, dc power systems, digital control, energy management, fuel cells, power conditioning, power system control.**

I. Introduction

A proton exchange membrane fuel cell (PEMFC) is a device that converts chemical fuels into electric power, with many advantages such as non-polluting emissions, high-current-output ability, high energy-density and low-operating temperatures. Additionally, this allows a fast start-up, high-efficiency and low weight and volume compared with other fuel cell types [1]–[3]. However, the relatively short lifespans of fuel cells represents a significant barrier for their commercialization in both stationary and mobile applications [4]–[11]. Therefore, a significant part of research in fuel cells focuses on prolonging their operational lives.

The PEMFC stack is a complex system that requires an auxiliary power-conditioning system to ensure safe, reliable and efficient operation under different operating conditions. The output characteristics of a PEMFC are limited by the mechanical devices used to maintain the air-flow within the cathode, either by using a compressor or a blower, hydrogen-flow within the anode through an adjustable valve command, temperature control using a cooling-fan, and the humidity of the air in the cell using a humidity-exchanger, as illustrated in Fig. 1. As the hydrogen, usually stored in a pressurized tank, is fed through a mechanical valve, air-flow can be considered as the main process that limits the PEMFC dynamics [12], [13]. As a consequence of this limitation, a load transient will cause a high voltage drop after a short time, which is a symptom of the oxygen starvation phenomena [14]–[17]. This operational condition is harmful for the FC because it accelerates the catalyst losses and the carbon-support corrosion [16], [18]–[20] and for this reason a FC is considered to be a slow dynamic response equipment with respect to the transient load requirements [21].

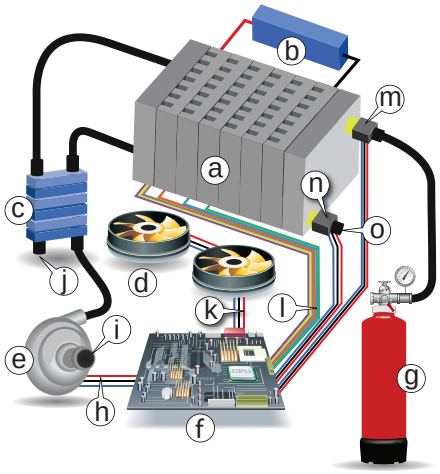

Fig. 1. PEM fuel cell system with main control subsystems: (a) fuel cell stack, (b) load, (c) humidifier, (d) fan system, (e) air pump, (f) fuel cell controller, (g) hydrogen tank, (h) air pump control, (i) inlet air, (j) exhaust air, (k) fan control, (l) monitored process variables, (m) inlet hydrogen valve, (n) hydrogen purge valve control, (o) hydrogen purge.

Different approaches to prevent the oxygen starvation phenomenon have been proposed in the literature. However, only two approaches have experimentally demonstrated efficacy for avoiding this phenomenon. The first approach focuses on the air flow rate control by means of a predictive control as a way of preventing oxygen starvation [12], [13], [22], [23]. The main drawback of this strategy is the air compressor dynamics can be slower than the load current variations. Hence, it is impossible to avoid peaks in the oxygen excess ratio after load

Manuscript received August 7, 2014; revised October 31, 2014 and December 5, 2014; accepted December 15, 2014

This work was supported by the Spanish Ministerio de Ciencia e Inovación under the projects CSD2009-00046, TEC2009-13172 and TEC2012-30952.

H. Ramírez-Murillo, J. Calvente, A. Romero and R. Giral are with the Departament d'Enginyeria Electrònica, Elèctrica i Automàtica, Escola Tècnica Superior d'Enginyeria, Universitat Rovira i Virgili, 43007 Tarragona, Spain.

C. Restrepo is with the Departamento de Ingeniería Eléctrica, Universidad Técnica Federico Santa María, Santiago, Chile.

Corresponding author. Email: javier.calvente@urv.cat. Postal Address: Avda. Països Catalans 26, Campus Sescelades, 43007, Tarragona, Spain. Fax: (+34)977559605. Telephone number: (+34)977297051.

This article has been accepted for publication in a future issue of this journal, but has not been fully edited. Content may change prior to final publication. Citation information: DOI 10.1109/TIE.2015.2395386, IEEE Transactions on Industrial Electronics

transients [13], which can lead to the appearance of oxygen starvation phenomena in the fuel cell. The second approach to avoid the oxygen starvation is hybridizing the fuel cell with an energy storage unit (batteries or ultracapacitors) or other auxiliary power sources for supporting the operation of the FC. This ensures a fast response to any load power transient. In the case of automotive hybrid powertrains, the fuel cell system can store large amounts of energy due its high energy density which provides the base power for constant speed driving for hours while the capacitors or batteries can pump into, or extract from, high power in microseconds or seconds which provides additional peak power during acceleration, high load operation and recover braking energy by regeneration as shown in the Ragone plot of Fig. 2. In addition, these hybrid systems can limit the slope of the current or the power generated by the FC by using current-controlled dc-dc converters and in this manner the oxygen starvation phenomenon can be avoided [24] and the system can operate with higher efficiency and extended operation compared to a purely fuel cell or battery/supercapacitor system [25]–[30]. For this reason, there is no need of modifying the FC internal control loops. Only the FC current maximum and minimum slew rate (SR) limits are required.

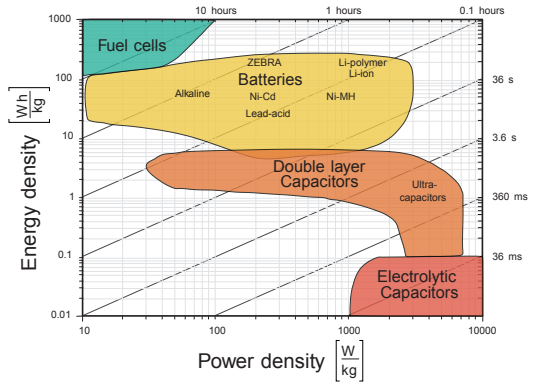

Fig. 2. Ragone plot which describes the energy storage technologies in terms of energy density and power density. Diagonal lines indicate the relative time to get the charge in or out of the device. Reprinted from [31] with permission from Elsevier.

In recent years, many configurations of a hybrid dc power conversion system relating to fuel cells and auxiliary storage device have been proposed for stationary and mobile applications in the literature. A mathematical analysis of efficiency of the commonly used series and parallel hybrid topologies is presented in [35]. A novel series-parallel hybrid (SPH) topology has been also proposed in this research work and it is illustrated in Fig. 3. This new topology exhibits a higher efficiency than the series or parallel hybrid topologies in non-regenerative operation independent of the load profile, because a part of power passes through only one converter, instead of all of the FC system converters. This advantage is very important for applications with an unknown load profile, however this topology presented major difficulties in its practical implementation with a high efficiency and an easy control design so far. The main challenges are described below.

The topology presented in Fig. 3 has been designed to

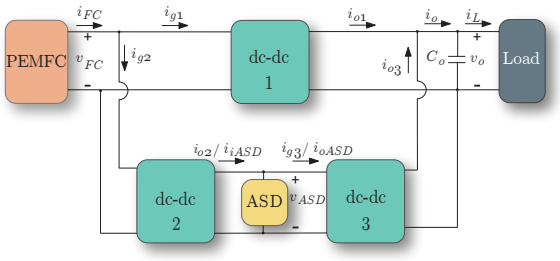

Fig. 3. Fuel Cell serial-parallel hybrid topology.

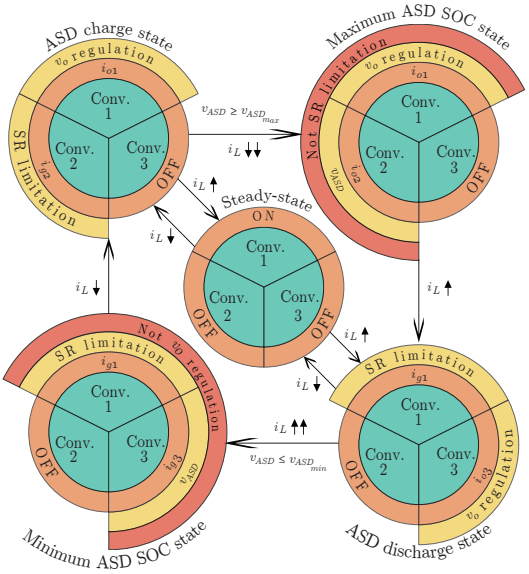

Fig. 4. Main states of the fuel Cell serial-parallel hybrid topology.

operate mainly in five different states. In the steady-state, the fuel cell is continuously transferring energy to the load by means of converter 1 and the other converters are not working as shown Fig. 4. From the steady-state, when a load increase appears, the FC system change to the ASD discharge state. In this case, converter 1 controls its input current i_{g1} with a slew rate limitation to avoid the oxygen starvation phenomenon, while the ASD provides the additional current to the load by means of converter 3. In this state converter 3 is controlling the dc bus voltage with a nested cascade loop by means of its output current i_{o3}. The system is kept in this state until the FC reaches the new value of the load current which changes back to the steady-state. If the load decreases, the system goes to the ASD charge state. The converter 1 controls the dc bus voltage and the converter 2 controls its input current to charge the ASD with the energy excess provided by the fuel cell. The three first states above correspond to the normal operation of the FC system, in which the ASD state of charge (SOC) is kept constant, but there are two additional protection states and correspond to the maximum and minimum ASD SOC. This states occurred when the load current decreases or increases too much so that the ASD SOC reaches its maximum or minimum value. The converter 2 must change its aim from controlling i_{g2} to i_{o2} during the ASD charge state, or the converter 3 changes its aim from controlling i_{o3} to i_{g3} during

This article has been accepted for publication in a future issue of this journal, but has not been fully edited. Content may change prior to final publication. Citation information: DOI 10.1109/TIE.2015.2395386, IEEE Transactions on Industrial Electronics

TABLE I
SUMMARY OF THE MAIN FC SERIAL-PARALLEL HYBRID SYSTEMS.

Presented in	Fuel cell range [V]	ASD type	Conv. 1 type	Conv. 2 type	Conv. 3 type	Output voltage v_0 [V]	Switching frequency [kHz]	Maximum load power [W]	Experimental Results
[32]	20 to 40	Lead-acid battery	Flyback	Boost	Flyback	200	20	360	✓
[33]	32 to 46	Lead-acid battery	SEPIC	Buck	SEPIC	200	20	1000	✓
[34]	25 to 38	Ultracapacitor	Boost	Flyback	Boost	48	Not specified	circa 1000	×
In this work	22 to 50	Aluminum electrolytic capacitor	Buck-boost	Buck-boost	Buck-boost	48	100	1000	✓

the ASD discharge state, respectively. The voltage v_{ASD} is limited by means this currents. After a long period of the system being in the ASD discharge state, with a power load consumption higher than the fuel cell can generate, the system changes to the minimum ASD SOC state. In this state the priority is to avoid an ASD deep discharge that could cause its lifespan reduction. This is why the output voltage v_o is not regulated during this state as can be seen in Fig. 4. During the minimum ASD SOC state, converter 3 changes its aim from controlling its output current to controlling its input current with an input current reference i_{gref3} equal to zero amperes. On the other hand, converter 2 is kept off to ensure a maximum power transfer from the fuel cell to the load. Once the fuel cell power generation is greater than the power load consumption the system changes to the ASD charge state as shown in Fig. 4. It is important to note that the minimum ASD SOC state is not a normal system operation state but a protection one. Since the ASD selected in this research work is an electrolytic capacitor, the maximum and minimum ASD SOCs can be limited properly by means its maximum and minimum voltages values (V_{ASDmax} and V_{ASDmin}).

In the design of the SPH topology will be used a modular converter so that it could be positioned in any location of the FC system of Fig. 3. The use of the same converter at the three positions in this FC system could reduce the costs and development time and could simplify the control tasks. In this case the converter and its controller should have the following features:

- A non-inverting step-up/step-down DC-DC converter characteristic. This would allow interfacing between unregulated voltage sources in the SPH topology such as fuel cells, capacitors, batteries, etc.
- High power conversion efficiency. This can significantly contribute to the efficiency of the whole system which is considered a topology that can achieve extremely high efficiency.
- A wide bandwidth to design fast controllers to protect the fuel cell from abrupt load changes. In addition, system control design becomes simpler and the ASD size can be reduced.
- Input and output currents regulation ability. This is because converter 2 requires input current control, converter 3 requires output current control and converter 1 requires both, input and output, current controllers.
- Ability to change its aim from controlling input current to controlling the output current, and vice-versa in a fast and smooth manner. This feature is very important to ensure converter 1 the different combinations between states shown in Fig. 4. In case of a sudden load change, the control aim of the converter 1 has to be immediately changed to controlling the input current to protect the fuel cell from an overload condition and gas-starvation phenomena.

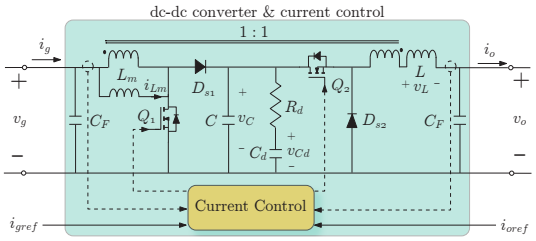

Fig. 5. Proposed modular buck-boost converter with its current control.

All above mentioned requirements can be fulfilled by the non-inverting buck-boost converter proposed in Fig. 5 [36]. Its advantageous features include high power conversion efficiency, wide bandwidth, the possibility of controlling either the input and output voltages or currents [37] and achieving fast and smooth transitions when changing the control objective from controlling the input current to control the output current and vice-versa [38]. This module has been used previously in a simple FC series hybrid topology [39]. The series-parallel hybrid topology challenges gave rise to the non-inverting buck-boost converter and it is now presented for the first time in the topology for which it was designed. The SPH topology has been already studied in previous works [32]–[34]. Table I lists the different configuration presented in the literature and the proposed in this work. The main contributions of this paper in comparison with the already existing SPH topologies are:

- The use of the same module for all the converters represents a reduction of the manufacturing times and costs. In addition, the modeling and control design tasks are also simplified.

This article has been accepted for publication in a future issue of this journal, but has not been fully edited. Content may change prior to final publication. Citation information: DOI 10.1109/TIE.2015.2395386, IEEE Transactions on Industrial Electronics

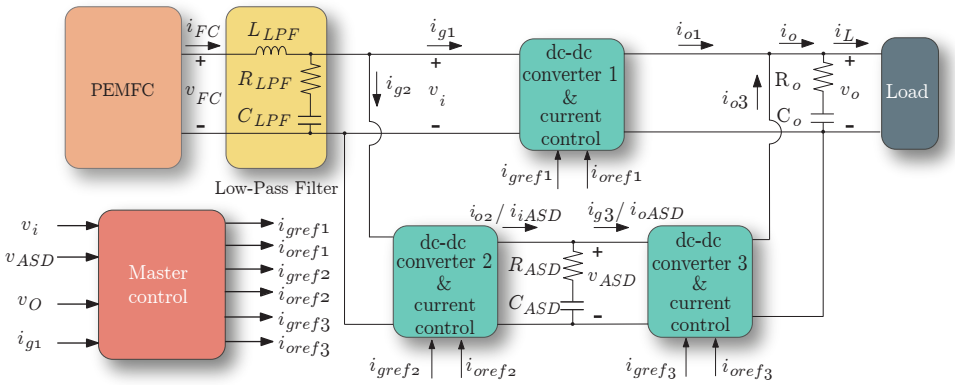

Fig. 6. FC serial-parallel hybrid topology circuit. The FC system elements are FC emulator, second order low-pass filter, modular buck-boost converter 1, 2 and 3, ASD capacitor C_{ASD}, dc bus capacitor C_o and load. The master control regulates the input/output port voltages from each converter by means of the current reference values.

- The boost converter used in [32] has startup problems. This issue is solved through the use of a buck converter in [32]. However, the nominal ASD value is within the range of the FC which could avoid the ASD charge at certain times. Both problems are overcome with the buck-boost converter presented in this paper.
- The module used in this paper has better efficiency than the flyback and SEPIC converters used in other works.
- Detailed information about the energy management algorithm design is given in this paper contrary to the work presented in other previous works [32]. Furthermore, the energy management in this paper is simpler than the one presented in [33] which depends of the battery state-of-charge.
- In the presented SPH topology in this article, the fuel cell slew rate limitation as a mechanism to avoid the oxygen starvation is included.
- In contrast to other works, the experimental and simulation results verifies the correct design of the proposed energy manegement. These experiments include the system startup and shutdown, and different load transients. Most of the works presented in the literature only show the fuel cell in steady-state.

This paper is organized as follows: Section II presents a detailed description of the energy management algorithm design. Simulations and experimental results are presented in Section III and, finally, the main conclusions of this paper are summarized in Section IV.

II. Energy Management Description

The circuit diagram implementation of FC serial-parallel hybrid topology shown in Fig. 3 is presented in Fig. 6. Its voltage, power control loops and protection specifications are listed in Table I of [39], [40], where V_{FCmin} and V_{FCmax} and P_{omax} have been changed into 26.0 V, 42.0 V and 1.2 kW, respectively, due to the FC emulator was replaced by a real PEMFC. We have chosen a 600 mF commercial electrolytic capacitor with an Equivalent Series Resistance (ESR) of 1 mΩ. This element was sized based on the energy that the electrolytic capacitor can absorb or deliver [39], [41]. The selection of this ASD eases the control of the SOC from this capacitor by means the ASD voltage regulation [39].

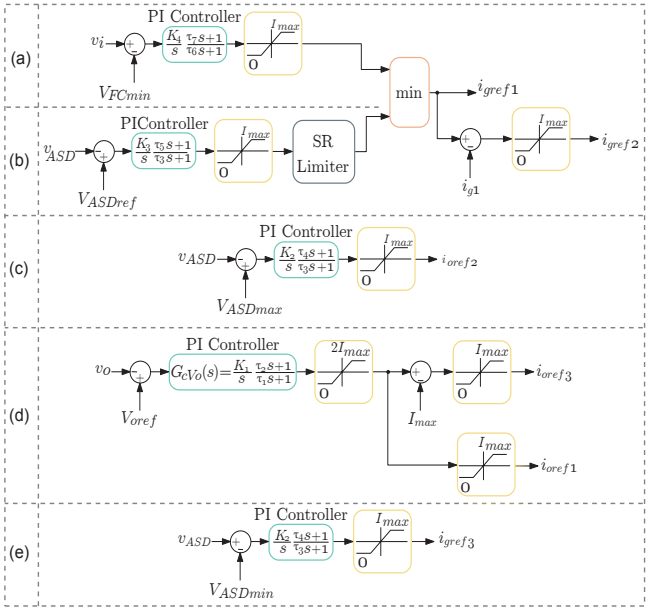

Fig. 7. FC serial-parallel hybrid system control and protection block diagrams: The FC minimum voltage V_{FCmin} and the ASD voltage reference V_{ASD} from (a) and (b) are limited and regulated by means of i_{gref1} and i_{gref2}. (c) ASD maximum voltage protection loop. (d) Output voltage v_o regulation loop and (e) ASD minimum voltage protection loop.

The master control shown in Fig. 7 has the following aims, among others: FC slope current limitation, FC and ASD voltage range protection, dc bus voltage v_o regulation at 48 V, maximum current limitation in each converter, and ensure a safe startup and shutdown of the system. This master control sends the current references to the analog current loops of each converter to regulate the different voltages of the system. The master control parameters are listed in Table II of [39], [40] and it has been implemented on a Texas Instruments TMS320F28335 DSC.

Fig. 8 shows the small-signal block diagram of the State Space Averaged (SSA) model of the modular buck-boost con-

This article has been accepted for publication in a future issue of this journal, but has not been fully edited. Content may change prior to final publication. Citation information: DOI 10.1109/TIE.2015.2395386, IEEE Transactions on Industrial Electronics

verter with its corresponding Average Current-mode Control (ACC) [38], which is an analogue PI controller with an additional pole. Additionally, the continuous control variable $u(t)$ is related with the duty cycles $d_1(t)$ and $d_2(t)$ of MOSFETs Q_1 and Q_2 in Fig. 5. For a small-signal analysis, they are related as follows:

$$\hat{u}(t) = \begin{cases} \hat{d}_1(t) & \text{for boost mode} \\ \hat{d}_2(t) & \text{for buck mode} \end{cases} \quad (1)$$

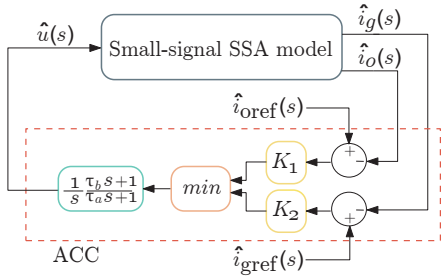

Fig. 8. Small-signal block diagram of the converter and the interaction between current loops.

The proposed modular buck-boost converter has two different models according to the required time scale: the first one is a dynamic model that allows to study the short-time transitions as shown in Fig. 5. The second one is a static model to make long-time simulations as can be seen in Fig. 9.

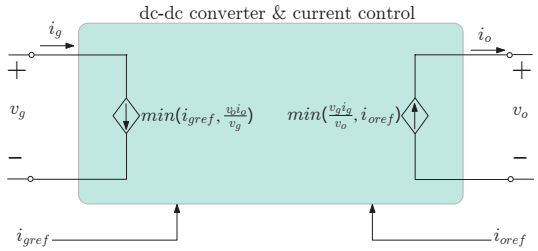

Fig. 9. Modular buck-boost converter block diagram to study long-time simulations.

The output capacitor C_o value of 2.35 mF with an ESR of 11.8 mΩ was selected following the output impedance criteria of [39]. The output voltage loop bandwidth value of 2.37 kHz was achieved by means of a digital sampling frequency of 100 kHz.

III. Simulation and Experimental Results

Some specific experiments are required to verify the correct performance of the FC SPH system. These experiments are the FC system's startup and shutdown and its operation under load transients, which are illustrated in subsections III-A and III-B, respectively. In all of these experiments a real Nexa fuel cell has been used. The Nexa PEMFC is a fully integrated system that produces unregulated dc power, up to 1200 W, from a supply of hydrogen and air.

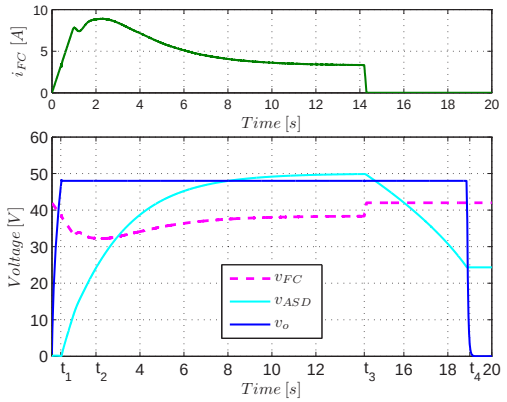

(a)

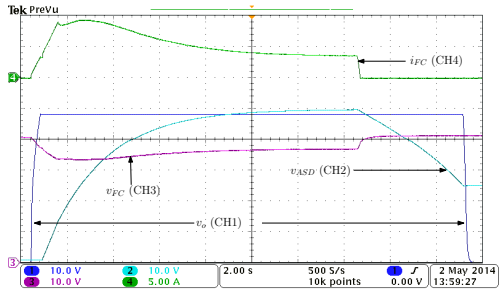

(b)

Fig. 10. FC system startup and shutdown with a constant resistance load of 20.3 Ω (a) PSIM simulation. (b) Experimental measurement. CH1: DC bus voltage v_o (10 V/div), CH2: ASD voltage v_{ASD} (10 V/div), CH3: FC voltage v_{FC} (10 V/div), CH4: FC current i_{FC} (5 A/div) and time base of 2 s.

A. FC hybrid System Startup and Shutdown.

This experiment studied the FC system's behavior during its startup and shutdown. Simulation results from Fig. 10(a) show how the fuel cell started up and the output capacitor began to charge until t_1, where v_o was then regulated at $V_{oref} = 48$ V by means i_{oref1} from the control loop of Fig. 7 (d). The figure shows how the FC current had an appropriate maximum SR, which corresponds to the control loop presented in Fig. 7 (b) by means i_{gref1} between 0 and t_1 and thus the FC current maximum SR value has been well limited by means i_{gref2}. At instant t_2, the capacitor reached V_{ASDmin} and continued charging until it reached its reference value V_{ASDref} of 50 V at t_3. After the corresponding Shutting down signal was applied at t_3, the fuel cell shut down with a correct current negative SR, and the output voltage v_o continued to be regulated by means i_{oref3} until the voltage capacitor decreased below V_{ASDmin} value, which occurred at t_4. The control loop active during this interval is the ASD minimum voltage protection loop shown in Fig. 7 (e). Finally, the master control regulates the minimum capacitor voltage from t_4 onwards. The simplified modular buck-boost converter from Fig. 9 was used in the simulation. The corresponding experimental result shown in Fig. 10(b) is in good agreement with the simulation. In the FC system's startup and shutdown experiment, and in the remaining ones, the V_{FCmin} and V_{ASDmax} protection loops of Figs. 7 (a) and (c) did not have to be activated by the

This article has been accepted for publication in a future issue of this journal, but has not been fully edited. Content may change prior to final publication. Citation information: DOI 10.1109/TIE.2015.2395386, IEEE Transactions on Industrial Electronics

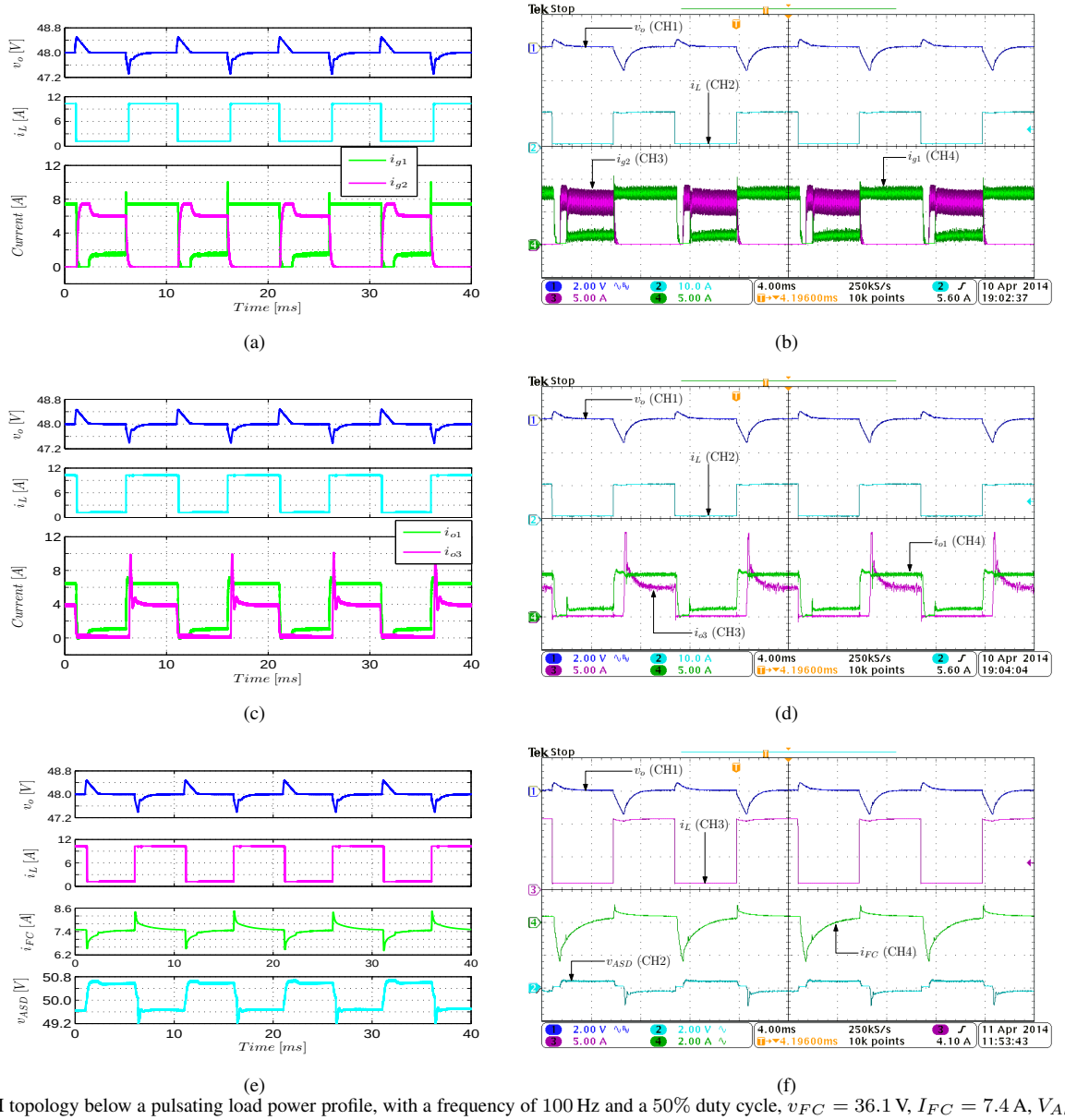

Fig. 11. SPH topology below a pulsating load power profile, with a frequency of 100 Hz and a 50% duty cycle, $v_{FC} = 36.1$ V, $I_{FC} = 7.4$ A, $V_{ASD} = 50$ V and $V_o = 48$ V as mean values. Figures (a), (c) and (e) are PSIM simulations. Figures (b), (d) and (f) correspond to experimental measurements. Output voltage v_o (2 V/div, AC coupling), load current i_L (5 or 10 A/div), input currents i_{g1} and i_{g2} (5 A/div), output currents i_{o1} and i_{o3} (5 A/div), fuel cell current i_{FC} (2 A/div, AC coupling), ASD voltage v_{ASD} (2 V/div, AC coupling) and the same time base of 4 ms.

master control. Although they were not included in this paper, the correct activation and performance of these protections were also tested.

B. FC hybrid System Operation Over Load Transients.

The second conducted experiment verified that the master control regulated in a satisfactory manner the capacitor voltage V_{ASD} at 50 V and the output voltage v_o at 48 V while the load resistance changes from 47.5 Ω to 4.7 Ω with a frequency of 100 Hz and a duty cycle of 50% as shown in Fig. 11. Output voltage v_o and load current i_L have been shown in all the figures to show that all of the experimental traces correspond to the same experiment. In the simulation, the switching model of the buck-boost converter presented in Fig. 5 was used. The experimental results presented in Fig. 11 are in good agreement with the simulation. Different current ripple values from i_{g1} and i_{g2} in Fig. 11(a) and Fig. 11(b) show the different operation points from converters 1 and 2, respectively. Initially, the system is in the steady-state of Fig. 4 and the FC energy is continuously transferred to the load and v_o is regulated at V_{oref} through i_{gref1} from Fig. 7 (d). Once i_L increases, the FC system is operating in the ASD discharge state, which means that the FC current maximum SR and dc bus voltage v_o are limited and regulated by means i_{gref1} and i_{oref3}, respectively. When the load current decreases, the SPH topology is operating in the ASD charge state. During this third state, FC current minimum SR and dc bus voltage v_o are limited and regulated by means i_{gref2} and i_{oref1}, respectively. Between the ASD charge and discharge states the FC system keeps the steady-state of Fig. 4 when the FC reaches the

This article has been accepted for publication in a future issue of this journal, but has not been fully edited. Content may change prior to final publication. Citation information: DOI 10.1109/TIE.2015.2395386, IEEE Transactions on Industrial Electronics

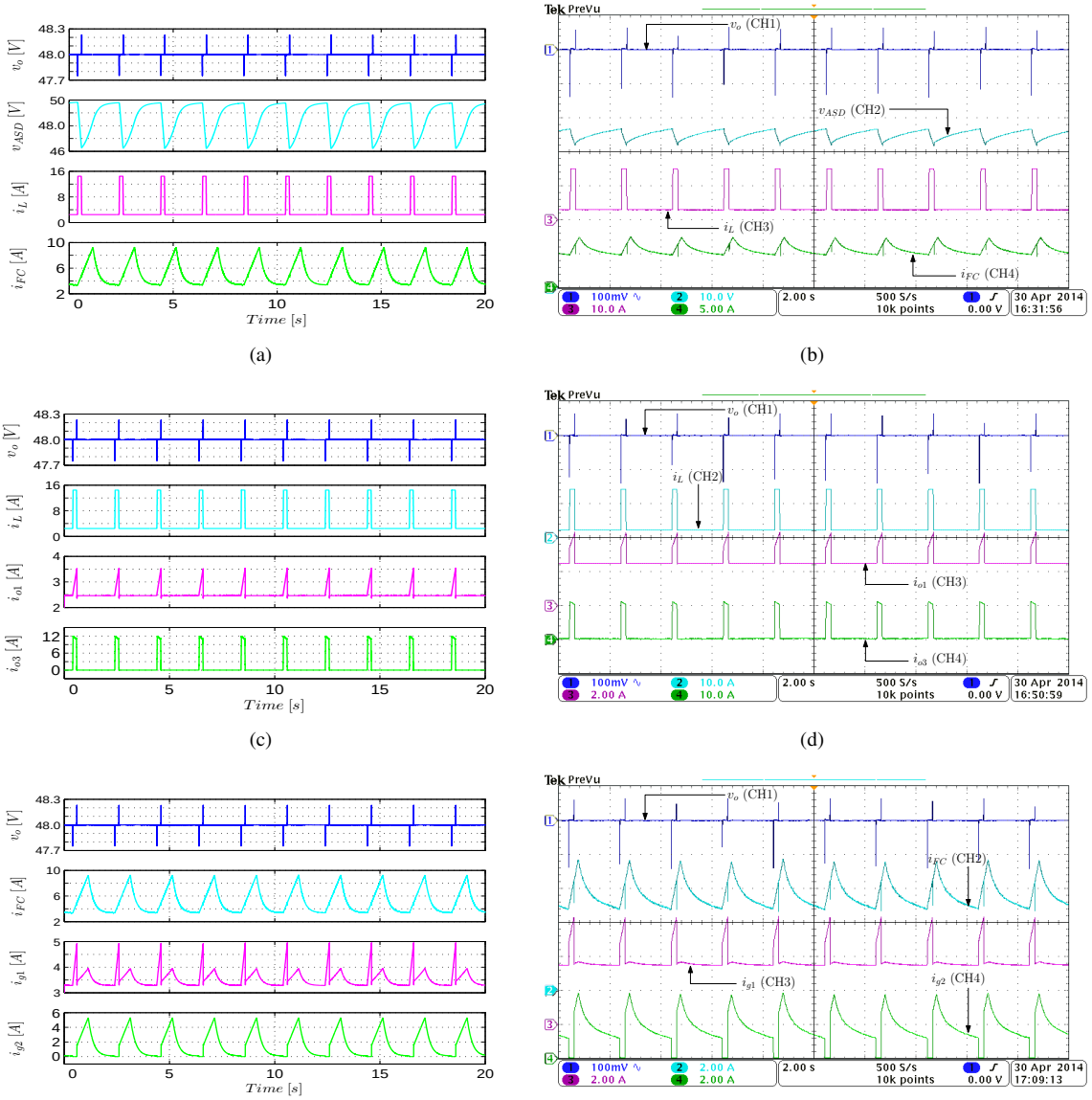

Fig. 12. SPH topology below a large load variations from 20.3 Ω to 3.3 Ω, with a frequency of 0.5 Hz and a 10% duty cycle that produce the ASD to charge and to discharge. Figures (a), (c) and (e) are PSIM simulations. Figures (b), (d) and (f) correspond to experimental measurements. Output voltage v_o (100 mV/div, AC coupling), load current i_L (10 A/div), input currents i_{g1} and i_{g2} (2 A/div), output currents i_{o1} and i_{o3} (2 A/div and 10 A/div, respectively), fuel cell current i_{FC} (2 or 5 A/div), ASD voltage v_{ASD} (10 V/div) and the same time base of 2 s.

new value of the load. Simulated and experimental output currents from converters 1 and 3 are provided by Fig. 11(c) and Fig. 11(b), respectively. Differences between simulation and experimental results of Fig. 11(e) and Fig. 11(f) are due to the delay in the startup from each dc-dc converter. This last oscillogram shows that an output current change Δi_o of 9.2 A caused a maximum output voltage transient Δv_o of 1.6 V. In addition, the capacitor voltage exhibited a peak ripple lower than 0.4 V. Also, as Fig. 11(f) shows, the fuel cell maximum current transient of 2.8 A.

The second experiment of this subsection tested the FC hybrid system is under large periodic load variations, which produced repetitive capacitor charging and discharging cycles. A step-like load variation from 20.3 Ω to 3.3 Ω with a frequency of 0.5 Hz and a duty cycle of 10% was applied to obtain the simulation and experimental results shown in Fig. 12. The simplified buck-boost converter model from Fig. 9 was used in the simulation. The maximum fuel cell power was 512 W, which is in agreement with the product of the FC parameters V_{FCmin} and I_{max} in [39], [40]. However, the large variations required a load peak power of 700 W, which produced a charge and discharge of the capacitor. Fig. 12 shows that the bus voltage and the fuel cell current were well regulated and limited during this demanding experiment. The figure also shows good agreement between the experimental data and the simulation results.

IV. Conclusion

A hybrid power system supplied by a PEMFC, an ASD and current controlled dc-dc converters has been simulated

and implemented on a 48-V, 1200-W dc bus. The energy management algorithm of this topology has been realized with a DSC TMS320F28335. Modular buck-boost converters have been used in this topology for regulating the system voltage loops by controlling their input/output currents through the appropriately limited reference values. Simulation and experimental results show a desired FC system behavior under short transients. The zero crossing saturation problem in the low-level analog current controllers could be addressed by means of implementing digital ones or using bidirectional buck-boost modules in future studies.

REFERENCES

[1] J. Larminie and A. Dicks, *Fuel Cell Systems Explained*, 2nd ed. Publisher Wiley, 2003.

[2] J. Correa, F. Farret, L. Canha, and M. Simoes, "An electrochemical-based fuel-cell model suitable for electrical engineering automation approach," *IEEE Trans. Ind. Electron.*, vol. 51, no. 5, pp. 1103 – 1112, Oct. 2004.

[3] J. Pukrushpan, A. Stefanopoulou, and H. Peng, "Control of fuel cell breathing," *IEEE Control Syst. Mag.*, vol. 24, no. 2, pp. 30 – 46, Apr. 2004.

[4] P. Thounthong and P. Sethakul, "Analysis of a fuel starvation phenomenon of a pem fuel cell," in *Power Convers. Conf., PCC*, Apr. 2007, pp. 731–738.

[5] D. Nelson, M. Nehrir, and V. Gerez, "Economic evaluation of grid-connected fuel-cell systems," *IEEE Trans. Energy Convers.*, vol. 20, no. 2, pp. 452 – 458, Jun. 2005.

[6] B. Wahdame, D. Candusso, X. Francois, F. Harel, M.-C. Pera, D. Hissel, and J. Kauffmann, "Analysis of a fuel cell durability test based on design of experiment approach," *IEEE Trans. Energy Convers.*, vol. 23, no. 4, pp. 1093 –1104, Dec. 2008.

[7] A. Dalvi and M. Guay, "Control and real-time optimization of an automotive hybrid fuel cell power system," *Contr. Eng. Practice*, vol. 17, no. 8, pp. 924 – 938, 2009.

[8] A. Mohammadi, D. Guilbert, A. Gaillard, D. Bouquain, D. Khaburi, and A. Djerdir, "Faults diagnosis between pem fuel cell and dc/dc converter using neural networks for automotive applications," in *Proc. 39th Annual Conf. IEEE Ind. Electron. Soc., IECON*, Nov. 2013, pp. 8186–8191.

[9] M. Youssef, M. Abu-Mallouh, M. Salah, M. Hamdan, and E. Abdel-Hafez, "A superior hybrid fuel cell vehicle solution for congested urban areas," in *Proc. 23rd IEEE International Symp. Ind. Electron., ISIE*, Jun. 2014, pp. 1600–1604.

[10] D. Guilbert, A. Mohammadi, A. Gaillard, A. N'Diaye, and A. Djerdir, "Interactions between fuel cell and dc/dc converter for fuel cell electric vehicle applications: Influence of faults," in *Proc. 39th Annual Conf. IEEE Ind. Electron. Soc., IECON*, Nov. 2013, pp. 912–917.

[11] A. Rathore and U. Prasanna, "Analysis, design, and experimental results of novel snubberless bidirectional naturally clamped zcs/zvs current-fed half-bridge dc/dc converter for fuel cell vehicles," *IEEE Trans. Ind. Electron.*, vol. 60, no. 10, pp. 4482–4491, Oct. 2013.

[12] W. Garcia-Gabin, F. Dorado, and C. Bordons, "Real-time implementation of a sliding mode controller for air supply on a PEM fuel cell," *J. Process. Contr.*, vol. 20, no. 3, pp. 325 – 336, 2010.

[13] J. Gruber, C. Bordons, and A. Oliva, "Nonlinear MPC for the airflow in a PEM fuel cell using a Volterra series model," *Contr. Eng. Practice*, vol. 20, no. 2, pp. 205 – 217, 2012.

[14] T. V. Nguyen and M. W. Knobbe, "A liquid water management strategy for PEM fuel cell stacks," *J. Power Sources*, vol. 114, no. 1, pp. 70 – 79, 2003.

[15] H. P. Jay T. Pukrushpan, Anna G. Stefanopoulou, *Control of fuel cell power systems: principles, modeling, analysis, and feedback design*, 1st ed. Springer, 2004.

[16] W. Schmittinger and A. Vahidi, "A review of the main parameters influencing long-term performance and durability of pem fuel cells," *J. Power Sources*, vol. 180, no. 1, pp. 1 – 14, 2008.

[17] J. Torreglosa, P. Garcia, L. Fernandez, and F. Jurado, "Predictive control for the energy management of a fuel-cellbatterysupercapacitor tramway," *IEEE Trans Ind. Informat.*, vol. 10, no. 1, pp. 276–285, Feb. 2014.

[18] A. Taniguchi, T. Akita, K. Yasuda, and Y. Miyazaki, "Analysis of electrocatalyst degradation in PEMFC caused by cell reversal during fuel starvation," *J. Power Sources*, vol. 130, no. 1-2, pp. 42 – 49, 2004.

[19] Z. Liu, L. Yang, Z. Mao, W. Zhuge, Y. Zhang, and L. Wang, "Behavior of PEMFC in starvation," *J. Power Sources*, vol. 157, no. 1, pp. 166 – 176, 2006.

[20] N. Yousfi-Steiner, P. Mootguy, D. Candusso, and D. Hissel, "A review on polymer electrolyte membrane fuel cell catalyst degradation and starvation issues: Causes, consequences and diagnostic for mitigation," *J. Power Sources*, vol. 194, no. 1, pp. 130 – 145, 2009.

[21] T. C. J. Restrepo, C. Konjedic and R. Giral, "A review of the main power electronics' advances in order to ensure efficient operation and durability of PEMFCs," *J. for Contr., Meas., Electron., Comput. and Commun., Automatika*, vol. 53, no. 2, pp. 184–198, 2012.

[22] J. Gruber, M. Doll, and C. Bordons, "Design and experimental validation of a constrained MPC for the air feed of a fuel cell," *Contr. Eng. Practice*, vol. 17, no. 8, pp. 874 – 885, 2009.

[23] A. Arce, A. del Real, C. Bordons, and D. Ramirez, "Real-time implementation of a constrained MPC for efficient airflow control in a PEM Fuel Cell," *IEEE Trans. Ind. Electron.*, vol. 57, no. 6, pp. 1892 –1905, Jun. 2010.

[24] C. Restrepo, C. A. Ramos-Paja, R. Giral, J. Calvente, and A. Romero, "Fuel cell emulator for oxygen excess ratio estimation on power electronics applications," *Comput. & Electr. Eng.*, vol. 38, no. 4, pp. 926–937, 2012.

[25] P. Rodatz, G. Paganelli, A. Sciarretta, and L. Guzzella, "Optimal power management of an experimental fuel cell/supercapacitor-powered hybrid vehicle," *Contr. Eng. Practice*, vol. 13, no. 1, pp. 41 – 53, 2005.

[26] P. Corbo, F. Corcione, F. Migliardini, and O. Veneri, "Experimental assessment of energy-management strategies in fuel-cell propulsion systems," *J. Power Sources*, vol. 157, no. 2, pp. 799 – 808, 2006.

[27] P. Thounthong, S. Rael, B. Davat, and I. Sadli, "A control strategy of fuel cell/battery hybrid power source for electric vehicle applications," in *Proc. 37th IEEE Annual Power Electron. Specialists Conf., PESC*, Jun. 2006, pp. 1 –7.

[28] C. Ramos-Paja, C. Bordons, A. Romero, R. Giral, and L. Martinez-Salamero, "Minimum fuel consumption strategy for PEM fuel cells," *IEEE Trans. Ind. Electron.*, vol. 56, no. 3, pp. 685 –696, Mar. 2009.

[29] K. Tsukahara and K. Kondo, "A study on methods to design and select energy storage devices for fuel cell hybrid powered railway vehicles," in *Proc. 39th Annual Conf. IEEE Ind. Electron. Soc., IECON*, Nov. 2013, pp. 4534–4539.

[30] J. Rurgladdapan, K. Uthaichana, and B. Kaewkham-ai, "Optimal li-ion battery sizing on pemfc hybrid powertrain using dynamic programming," in *Proc. 8th Annual Conf. IEEE Ind. Electron. Appl., ICIEA*, Jun. 2013, pp. 472–477.

[31] Q. Cai, D. Brett, D. Browning, and N. Brandon, "A sizing-design methodology for hybrid fuel cell power systems and its application to an unmanned underwater vehicle," *J. Power Sources*, vol. 195, no. 19, pp. 6559 – 6569, 2010.

[32] W. T. Yan, L. S. Yang, C. Hong, T. Liang, J. F. Chen, and H. T. Yang, "Fuel cell and battery hybrid supplied power system," in *Proc. International Conf. IEEE Electr. Machines and Syst., ICEMS*, Oct. 2008, pp. 2676–2680.

[33] A.-C. Hua and B.-y. Tsai, "Design of a wide input range dc/dc converter based on sepic topology for fuel cell power conversion," in *Proc. International Power Electron. Conf., IPEC*, 2010, pp. 311–316.

[34] B. Sami, B. Abderrahmen, and C. Adnane, "Design and dynamic modeling of a fuel cell/ultra capacitor hybrid power system," in *Proc. International Conf. IEEE Electr. Eng. Softw. Appl., ICEESA*, Mar. 2013, pp. 1–7.

[35] C. Ramos-Paja, A. Romero, R. Giral, J. Calvente, and L. Martinez-Salamero, "Mathematical analysis of hybrid topologies efficiency for PEM fuel cell power systems design," *International J. Electr. Power & Energy Syst.*, vol. 32, no. 9, pp. 1049–1061, 2010.

[36] C. Restrepo, J. Calvente, A. Cid-Pastor, A. Aroudi, and R. Giral, "A noninverting buck-boost dc-dc switching converter with high efficiency and wide bandwidth," *IEEE Trans. Power Electron.*, vol. 26, no. 9, pp. 2490–2503, Sept. 2011.

[37] C. Restrepo, J. Calvente, A. Romero, E. Vidal-Idiarte, and R. Giral, "Current mode control of a coupled-inductor buck-boost dc-dc switching converter," *IEEE Trans. Power Electron.*, vol. 27, no. 5, p.2536–2549, 2011.

[38] C. Restrepo, T. Konjedic, J. Calvente, M. Milanovic, and R. Giral, "Fast transitions between current control loops of the coupled-inductor buck-boost dc-dc switching converter," *IEEE Trans. Power Electron.*, vol. 28, no. 8, pp. 3648–3652, Aug. 2013.

[39] H. Ramirez-Murillo, C. Restrepo, J. Calvente, A. Romero, and R. Giral, "Energy management dc system based on current-controlled buck-boost

modules," *IEEE Trans. Smart Grid*, vol. 5, no. 5, pp. 2644–2653, Sept. 2014.

[40] H. Ramirez-Murillo, J. Calvente, A. Romero, R. Giral, and C. Restrepo, "Energy management of a fuel cell serial-parallel hybrid system," in *Proc. 11th International Multi-Conf. IEEE Syst., Signals Devices, SSD*, Feb. 2014, pp. 1–6.

[41] J. Pegueroles-Queralt, F.D. Bianchi, and O. Gomis-Bellmunt, "A Power Smoothing System Based on Supercapacitors for Renewable Distributed Generation," *IEEE Trans. Ind. Electron.*, vol. 62, no. 1, pp. 343 –350, Jan. 2015.

Harrynson Ramírez-Murillo (S'14) recieved the Ingeniero Electricista and Master en Ingeniería Eléctrica degrees from the Universidad Tecnológica de Pereira (UTP), Pereira, Colombia, in 2007 and 2010, respectively, and the master en Ingeniería Electrónica from the Universitat Rovira i Virgili (URV) de Tarragona, Tarragona, Spain, in 2011, where is currently toward the Ph.D. degree with the Departamento d'Enginyeria Electrònica, Elèctrica i Automàtica (DEEEA). His main research interests include fuel cell, converters design, control systems and power conditioning for dc systems.

Carlos Restrepo received the Bachelor degree (with honors) and the Master degree in electrical engineering in 2006 and 2007, respectively, from the Universidad Tecnológica de Pereira, Colombia, and the Master degree and the Ph.D. (with honors) degree in electronic engineering from the Universitat Rovira i Virgili de Tarragona, Tarragona, Spain, in 2008 and 2012, respectively.

He was a visiting scholar at the Faculty of Electrical Engineering and Computer Science, University of Maribor, Slovenia, in 2011. During 2013 and 2014, he was a Postdoctoral Researcher with the Electrical Power Processing Group, Delft University of Technology, Delft, The Netherlands. He is currently a Professor with the Departamento de Ingeniería Eléctrica, Universidad Técnica Federico Santa María, Santiago de Chile, Chile. His main research interests include modeling and emulator design for fuel cells, design and digital control of switched converters, and offshore wind farm integration into the power systems.

Javier Calvente (S'94-M'03) received the Ingeniero de Telecomunicación degree and the Ph.D. degree from the Universitat Politècnica de Catalunya (UPC), Barcelona, Spain, in 1994 and 2001, respectively. He was a visiting scholar with Alcatel Space Industries, Toulouse, France, in 1998. He is currently an Associate Professor with the Departamento d'Enginyeria Electrònica, Elèctrica i Automàtica, Universitat Rovira i Virgili (URV), Tarragona, Spain, where he is working in the fields of power electronics and control systems.

Alfonso Romero (S'97-M'02) received the Ingeniero de Telecomunicación degree and the Ph.D. degree from the Universitat Politècnica de Catalunya (UPC), Barcelona, Spain, in 1994 and 2001, respectively. He is currently an Associate Professor with the Departament d'Enginyeria Electrònica, Elèctrica i Automàtica, Escola Tècnica Superior d'Enginyeria, Universitat Rovira i Virgili, Tarragona, Spain, where he is working in the field of power electronics and instrumentation for renewable energy and distributed generation systems.

Roberto Giral (S'94-M'02-SM'10) received the B.S. degree in Ingeniería Técnica de Telecomunicación, the M.S. degree in Ingeniería de Telecomunicación, and the Ph.D. (with honors) degree from the Universitat Politècnica de Catalunya, Barcelona, Spain, in 1991, 1994, and 1999, respectively. He is currently an Associate Professor with the Departament d'Enginyeria Electrònica, Elèctrica i Automàtica, Escola Tècnica Superior d'Enginyeria, Universitat Rovira i Virgili, Tarragona, Spain, where he is working in the field of power electronics.